

UNIVERSITY OF MICHIGAN  
DEPARTMENT OF MECHANICAL ENGINEERING  
CAVITATION AND MULTIPHASE FLOW LABORATORY

Report No. UMICH 014571-1-T

(Mod. 1)

INVESTIGATIONS OF SECONDARY LIQUID PHASE STRUCTURE  
IN STEAM WAKE

(submitted to ASME)

by

S. Krzeczowski  
W. Kim  
F. G. Hammitt  
J-B. Hwang

Supported by: National Science Foundation Grant  
Nos. ENG 75-2315 and GK-40130  
and National Academy of Sciences  
(with cooperative program with the  
Polish Academy of Sciences)

June, 1976

## List of Figures

1. Schematic Diagram of the University of Michigan Steam Tunnel (3502)
2. Schematic of Test Section and the Position of Camera and Flash (836)
3. Photograph of Liquid Film Disintegration into Droplets at the Trailing Edge,  $M = 0.35$ ,  $q = 5 \text{ cm}^3/\text{cm-min.}$  (838a)
4. Photograph of Liquid Film Disintegration into Droplets at the Trailing Edge,  $M = 0.55$ ,  $q = 25 \text{ cm}^3/\text{cm-min.}$  (838b)
5. Maximum Droplet Size as a Function of the Distance from the Trailing Edge at Three Mach Numbers (843)
6. The Weber Number of Maximum Droplets Far Downstream from the Trailing Edge (844)
7. Droplet Size Distribution Function at  $M = 0.55$ ,  $x = 2.5 \text{ cm}$  and  $x = 4.0 \text{ cm}$  (846)
8. Droplet Mass Distribution Function at  $M = 0.55$ ,  $x = 2.5 \text{ cm}$  and  $x = 4.0 \text{ cm}$  (848)

## ABSTRACT

The disintegration of condensate film deposited on a stationary steam turbine blade has been studied photographically under various flow conditions. The maximum size of secondary droplets was found to be dependent on steam velocity and distance from the trailing edge, but seems to be relatively independent of film thickness. Size and mass distributions were determined as functions of distance and steam velocity.

## ACKNOWLEDGMENTS

The financial support of this investigation is provided by National Science Foundation Grants No. ENG 75-2315 and GK-40130. The authors are indebted to Professor Jerzy Krzyzanowski, Institute of Fluid Machinery, Polish Academy of Sciences, Gdansk, Poland, for the preliminary design of the facility and constant helpful suggestions.

## INTRODUCTION

The erosion, by condensate droplets, of rotor blades in the low pressure stages is a limiting factor of steam turbine design.

We must investigate the following phenomena in order to gain a better understanding of the erosion process.

1. Condensation of steam downstream of the Wilson Line.
2. Settling of small primary droplets ( $\sim 0.05$  mm) and formation of liquid film on the standard blade.
3. The motion of liquid film and subsequent disintegration into large secondary droplets ( $\sim 1$  mm) due to aerodynamic and centrifugal forces.
4. Collision of liquid droplets with rotor blades and methods of preventing erosion damage.

This investigation deals specifically with the third category of problems. As primary droplets accumulate, a thin liquid film forms on the stationary blade, it travels with main steam stream, with slower velocity and possibly breaks up into rivulets, if the film is thin enough, due to surface tension and aerodynamic forces. Liquid film or rivulets will eventually disintegrate into secondary droplets after leaving the blade.

The sizes of secondary droplets are approximately four orders of magnitude larger than that of primary droplets. Based on a theoretical approach, Kryzanowski estimated that the maximum droplet size present in the last stage of a steam turbine was about 300  $\mu$ m. Droplets up to 1 mm. diameter were detected experimentally by other investigators (2,3).

The main objective of this <sup>investigation</sup> is to find the relationship between secondary droplet stream structure and flow conditions. In order to study the formation of secondary droplets, and to find the factors affecting the droplet stream structure, condensate film has been created on a simulated stationary blade by feeding water through a thin slit at the leading edge of the blade.

## EXPERIMENTAL EQUIPMENT USED

Figure 1 is a schematic representation of our experimental facility. The pertinent flow parameters are as below:

$$(p_3)_{\max} = 3.75 \text{ psia} = 0.258 \cdot 10^5 \text{ N/m}^2 \quad (\text{saturated steam})$$

$$p_4 = 2.55 \text{ psia} = 0.175 \cdot 10^5 \text{ N/m}^2$$

Maximum Mach Number,  $M \approx 0.75$ .

The test section is located after a stilling tank which is supplied with low pressure steam from the laboratory heating supply ( $\sim 5$  psig, 0.9 quality). A diffuser then guides the steam to a jet-cooled condenser. The test section is of plexiglas, so that the liquid droplets downstream, as well as the liquid film upon the inserted flat plate, can be easily observed. This plate, which simulates a turbine fixed blade, is located inside the test section (Fig. 2). A thin liquid film was obtained upon the blade by means of a slot placed near the leading edge. Water flow-rate was measured by a flow meter, and liquid film thickness by means of the electrical resistance ↗

gage method (5), (6), using four gages in the plate surface.

The flow rate and liquid film thickness were as follows:

$$\dot{q} = 2.5 - 10 \text{ cm}^3 / (\text{cm} \cdot \text{min})$$

$$h = 50 - 250 \text{ } \mu\text{m}$$

The liquid film on the plate appeared first to disintegrate into liquid filaments, and next into "secondary" droplets (Fig. 3). These then pass downstream in the aerodynamic wake, still being disintegrating due to the increasing aerodynamic forces, since the velocity of the wake increases with distance downstream from the trailing edge.

This liquid-phase behavior was studied photographically.

The camera was located as close as possible to the test section, producing a magnification of  $\sim 2.4x$ . A light flash duration of  $\sim 1 \mu\text{s}$  was used, with light source perpendicular to camera axis (Fig. 2). This arrangement was most suitable as pictures so taken were sharp and with good contrast. Figures 3-4 are typical pictures. Full details are included elsewhere (7).

Droplet size measurement capability was, however, limited to droplets above  $\sim 50 \mu\text{m}$  diameter because of limited optical resolution of the camera and film. Smaller droplets had too great velocity to be recorded with the available  $1 \mu\text{s}$  flash duration. These limitations proved most significant at high Mach number ( $M \sim 0.75$ ), and relatively long distances downstream of the trailing edge.

We hope to develop another method for small droplets well downstream and at high Mach number. This method will be based

on laser light scattering from small particles, and should be useful for the measurement of  $1 \sim 20 \mu\text{m}$  droplets.

#### RESULTS OF THE EXPERIMENT

Because of the erosion threat to turbine blading, information of maximum droplet size is important. Many photographs ( $\sim 300$ ) have been made at three Mach numbers;

$$M = 0.35; 0.55; 0.75$$

and at three values of the flow rate:

$$\dot{q} = 2.5; 5.0; 10.0 \quad \text{cm}^3/(\text{cm} \cdot \text{min}).$$

Several relationships have been obtained. These are presented in Figure 5. All large droplets provide data points on these graphs according to their distance downstream in the aerodynamic wake (x-coordinate). The relationship between maximum droplet size and distance downstream,  $D_{\text{max}} = f(x)$ , is established as a limiting line above the area of the data points. This function has been shown as a belt because the process of liquid phase disintegration is very non-uniform.

The function  $D_{\text{max}} = f(x)$  decreases with distance  $x$  until  $x \approx 20$  cm and then remains essentially constant. It is independent of liquid flow rate for this experiment. However, the shape of the curves depends very strongly on the Mach number (Fig. 5).

To allow application of these results for other conditions, a more universal relationship has been generated. Using the results of Fig. 5, and transforming them into a dimensionless function of Weber number,

$$We_{\text{max}} = f(M),$$

the relationship of Fig. 6 was obtained. Here

$$We_{\max} = \frac{\rho \cdot V_{\infty}^2 \cdot D_{\max}}{\sigma}$$

$\sigma$  = surface tension

$D_{\max}$  = maximum droplet size, from center of data scatter, at distance  $x = 22$  cm, assuming maximum droplet size to be approximately constant for distances longer than  $x = 22$  cm

$V_{\infty}$  = the velocity of the steam outside of the aerodynamic wake.

Results obtained by other authors are also presented, i.e., Weigle and Severin (8), using an air tunnel, and Valha from a steam tunnel (9).

To obtain further information on liquid droplet stream structure, still another approach was applied. Based on several droplet pictures (eg. Figs 3-4) a droplet size distribution function has been established.

This function is defined as follows:

$$F(d) = \frac{N(d)}{N} \cdot \frac{1}{\Delta d}$$

where:

$d$  = droplet size

$\Delta d$  = droplet size interval ( $\Delta d = 200 \mu\text{m}$  for presented experiment)

$N(d)$  = average number of droplets of the size enclosed in the region  $(d - \frac{\Delta d}{2}, d + \frac{\Delta d}{2})$ ,

$N$  = average total number of the droplets visible in the test area.

In order to obtain the above function, droplets visible on the picture were counted according to their sizes (using a magnifying glass with scale). Consequently, the droplet size distribution



function was used to establish a droplet mass distribution function:

$$R(m) = \frac{m(d)}{m} \frac{1}{\Delta d} = \frac{\sum_{i=1}^n d_i^3 \cdot N(d_i)}{\sum_{i=1}^n d_i^3 N(d_i)} \frac{1}{\Delta d} = \frac{\sum_{i=1}^n d_i^3 F(d_i)}{\sum_{i=1}^n d_i^3 F(d_i)} \frac{1}{\Delta d}$$

where:

$m(d)$  = average mass of droplets of the size enclosed in the region  $(d - \frac{\Delta d}{2}, d + \frac{\Delta d}{2})$

$m$  = average total mass of the droplets visible in the test area.

$$n = \frac{d_{\max}}{\Delta d}$$

Both functions were normalized so that the integral equals unity.

The results of the experiment reduced to size and mass distribution functions are shown on Figs. 7-8 for the following values of the Mach number:

$$M = 0.35$$

$$M = 0.55 *$$

To be sure, both functions are being changed according to the distance  $x$ ; the ratio of large droplets decreases, and the ratio of small droplets increases. The same effect takes place as Mach number increases. The highest probability of droplets occurring (the maximum of the function of probability density) is shown below in the conclusions.

\*It was impossible to obtain any droplet size mass distribution function at  $M = 0.75$  due to limitations of the photographic system. The same difficulty appeared for long distances ( $X > 5$  cm) from the trailing edge.

## CONCLUSIONS

1. The maximum droplet size function  $D_{\max} = g(x, M)$ , decreases with the distance  $x$  and Mach number  $M$ .  $D_{\max}$  becomes constant for distance  $x \geq 22$  cm. In this region, maximum droplet size varies with Mach number.

$$\begin{array}{ll} M = 0.35; & D_{\max} = 750 \text{ } \mu\text{m} \\ & 0.55; & 500 \text{ } \mu\text{m} \\ & 0.75; & 250 \text{ } \mu\text{m} \end{array}$$

The variation of  $D_{\max}$  with respect to  $x$  and  $M$  proved to be different than estimated theoretically from the steam velocity distribution in the aerodynamic wake and the assumed critical Weber number, ( $We = 13$ ) (1). Droplet diameter here measured is at least twice that estimated before.

2. The critical value of the Weber number

$$We = \frac{\rho \cdot V_{\infty}^2 D_{\max}}{\sigma}$$

has been estimated as follows:

$$\begin{array}{ll} M = 0.35 & We \cong 30 \\ M = 0.5; 0.75; & We \cong 45 \end{array} \quad (\text{Fig. 6})$$

3. The most probable droplet size to appear in the aerodynamic wake, in the vicinity of the trailing edge ( $x = 2.5$  to  $4$  mm), according to the size distribution function is:

$$\begin{array}{ll} M = 0.35; & d \cong 250 \text{ } \mu\text{m} \\ M = 0.55; & d \cong 133 \text{ } \mu\text{m} \end{array}$$

and according to the mass distribution function:

$$\begin{array}{ll} M = 0.35; & d \cong 500 \text{ } \mu\text{m} \\ M = 0.55; & d \cong 475 \text{ } \mu\text{m} \end{array}$$

4. There is no significant influence of (water) liquid film flow rate ( $\dot{q} \cong 10 \text{ cm}^3/\text{cm.s}$ ) on the maximum droplet size  $D_{\max}$ , and on the droplet size and mass distribution function  $F(d)$ ,  $R(m)$ .

REFERENCES

1. Puzyrewski, R. and Krzeczowski, S., "Some Results of Investigations on Water-Film Break-Up and Motion of Water Drops in Aerodynamic Trail," IFFM Trans., 29-31, 1966, Gdansk, Poland.
2. Christie, D. G., and Haywood, G. W., "Observation of Events Leading to the Formation of Water Drops Which Cause Turbine Blade Erosion," Phil. Trans. Roy Soc., 260 SA, No.1110, London, 1966.
3. J. P. Faddeev, "Structure of Erosion Inducing Streams of Droplets in Axial Clearance of Low-Pressure Part of the Turbine", Proc. of the III Conf. on Steam Turbine of Great Output, Prace IMP-PAN, Gdansk, Poland, 1975.
4. Krzyzanowski, J., "Wet-Steam Tunnel Facility-Design and Program of Investigations", ORA Report No. UMICH 03371-18-T, Univ. of Mich, Ann Arbor, Mich., 1972.
5. Puzyrewski, R. and Jasinski, R., "Measurement of the Thickness of Thin Water Films by Resistance Method," IFFM - Trans. No. 26, 1965, Gdansk, Poland.
6. Mikielwicz, J., Hammitt, F. G., "Generalized Characteristics of Electrical Conductance Film Thickness Gauges," Proc. 6th Steam Turbines Large Output, Pilsen, Czech. 16-19, Sept. 1975.
7. Krzeczowski, S., Kim, W., Hammitt, F. G., and J-B Hwang, "Investigation of Secondary Liquid Phase Structure in Steam Wake," DRDA Rept. No. UMICH 014571-I-T, June, 1976.
8. Weigle, B. and Severin, H., "Badania nad wplywem predkosci fazy gazowej na strukture strumienia kropel i jego oddzialywanie na efekty erozji," IFFM Bulletin, Nr arch. 273/71, Gdansk, 1971.
9. Valha, J., "Liquid Film Disintegration on the Trailing Edges of Swept Bodies", Strojnický Casopis, Ročník XXI, číslo 3, 1970.
10. Valha, J., Rozpad kapalinových filmuo na odtokove hrane profilu při vysokých rychlostech, Proceedings of the Skoda Conference, Plzen, 1972.

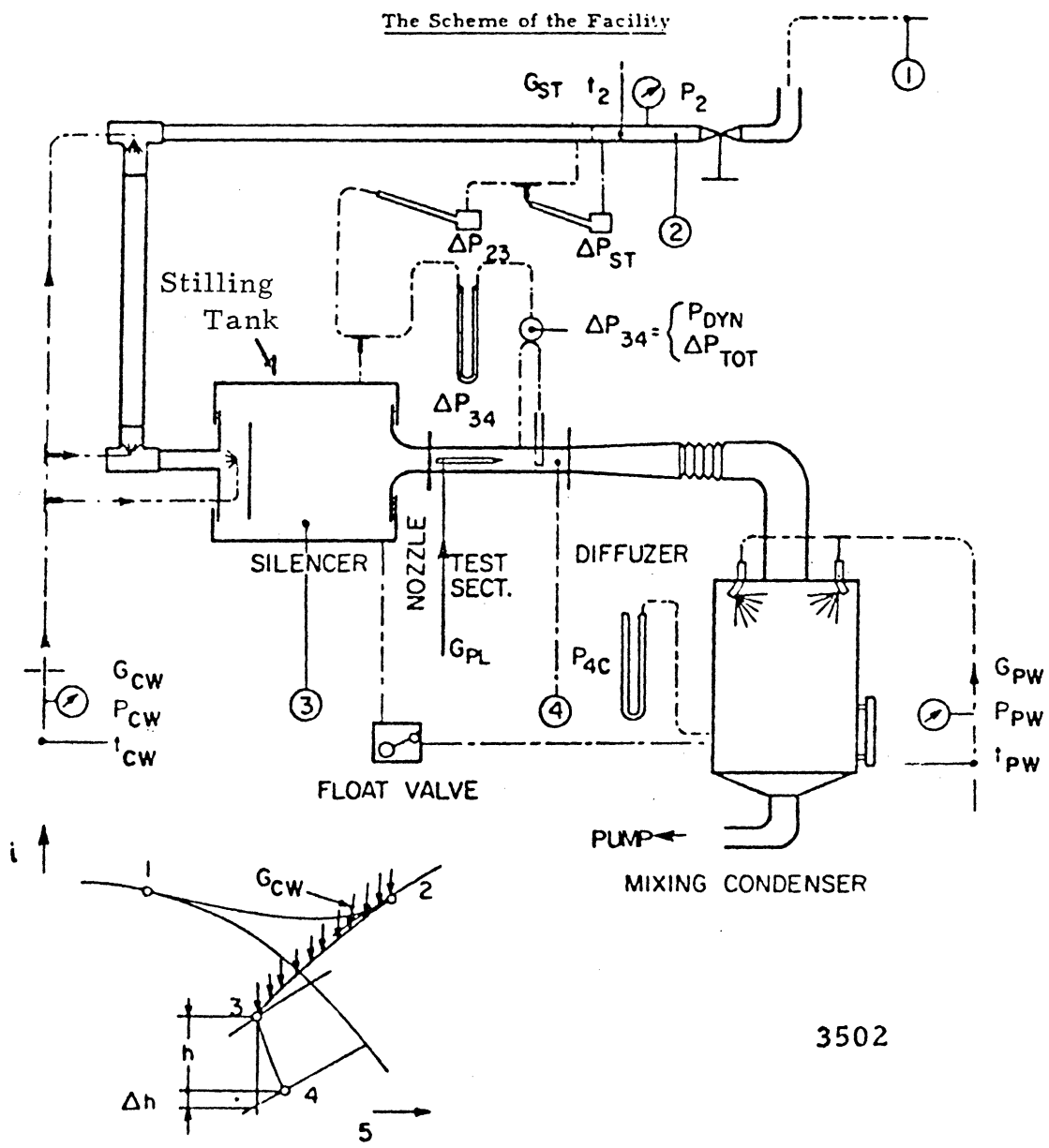


Figure 1 - Schematic Diagram of the University of Michigan Steam Tunnel

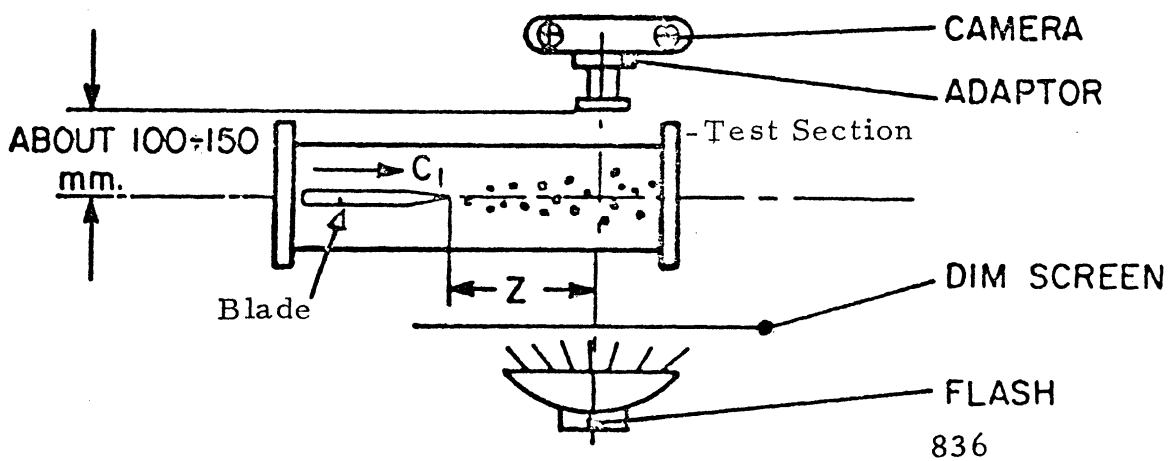


Figure 2 - Schematic of Test Section and the Position of Camera and Flash

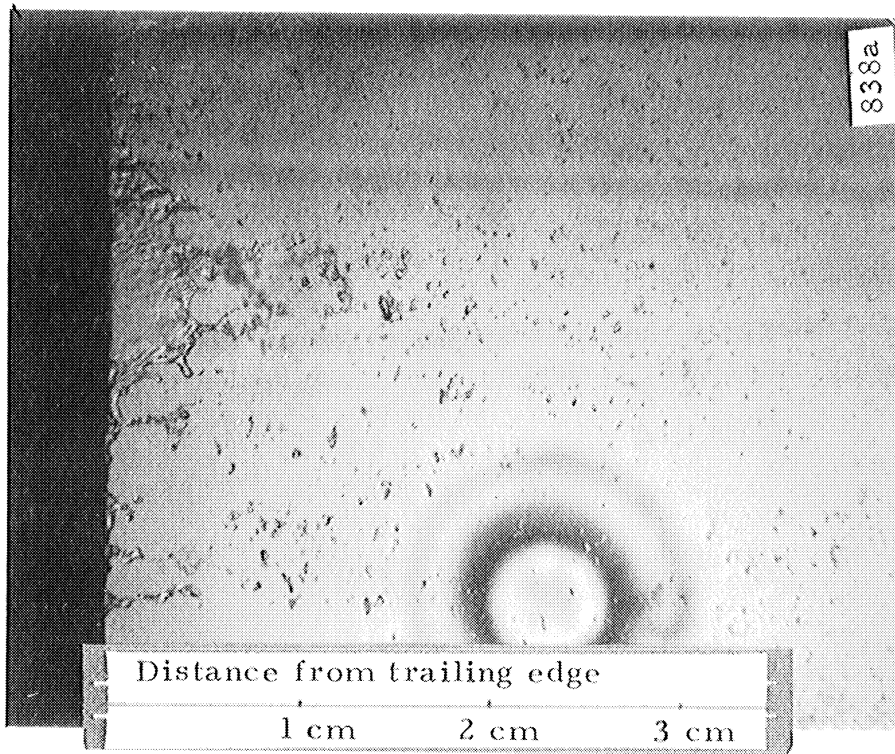


Figure 3 - Photographs of Liquid Film Disintegration into Droplets at the Trailing Edge,  $M = 0.75$ ,  $q = 5 \text{ cm}^3/\text{cm}\cdot\text{min.}$

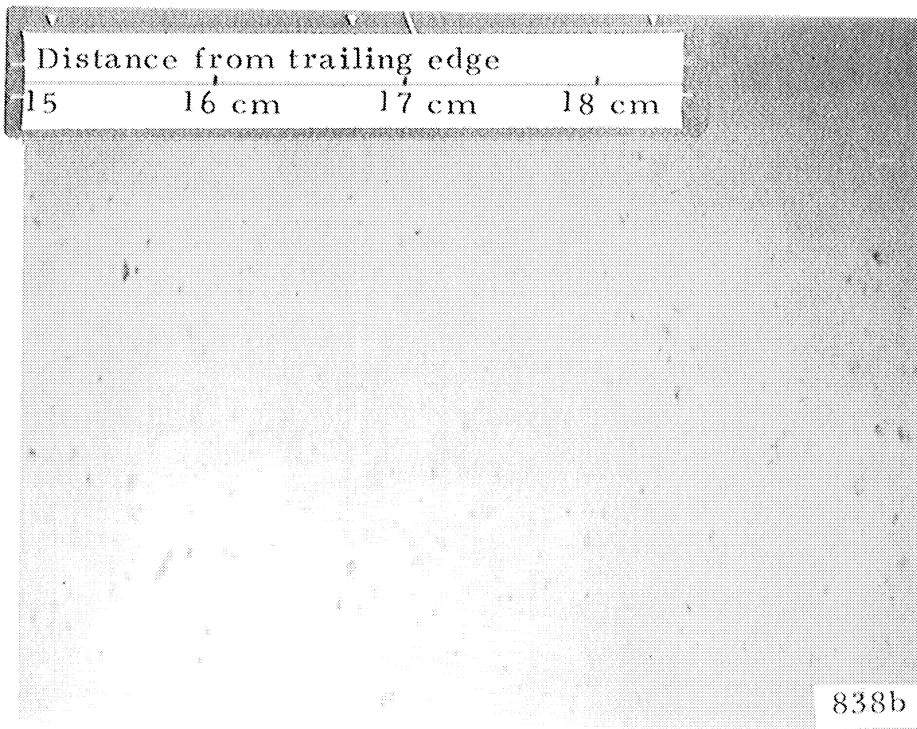


Figure 4 - Photographs of Liquid Droplets Distribution in Downstream Flow,  $M = 0.35$ ,  $q = 10 \text{ cm}^3/\text{cm}\cdot\text{min.}$ ,  $X = 14 \text{ cm}$

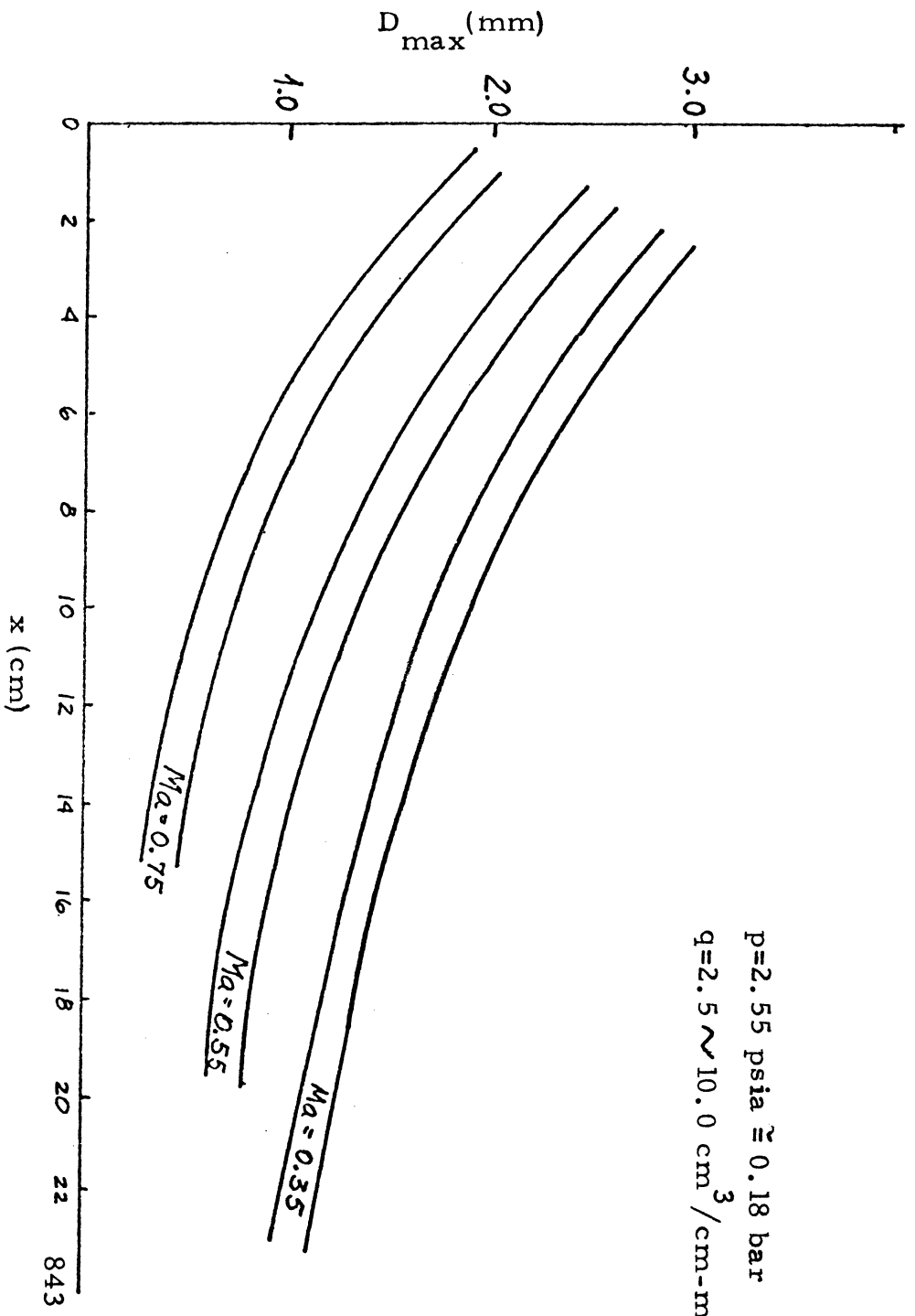


Figure 5 - Maximum Droplet Size as a Function of the Distance From the Trailing Edge at three Mach Numbers

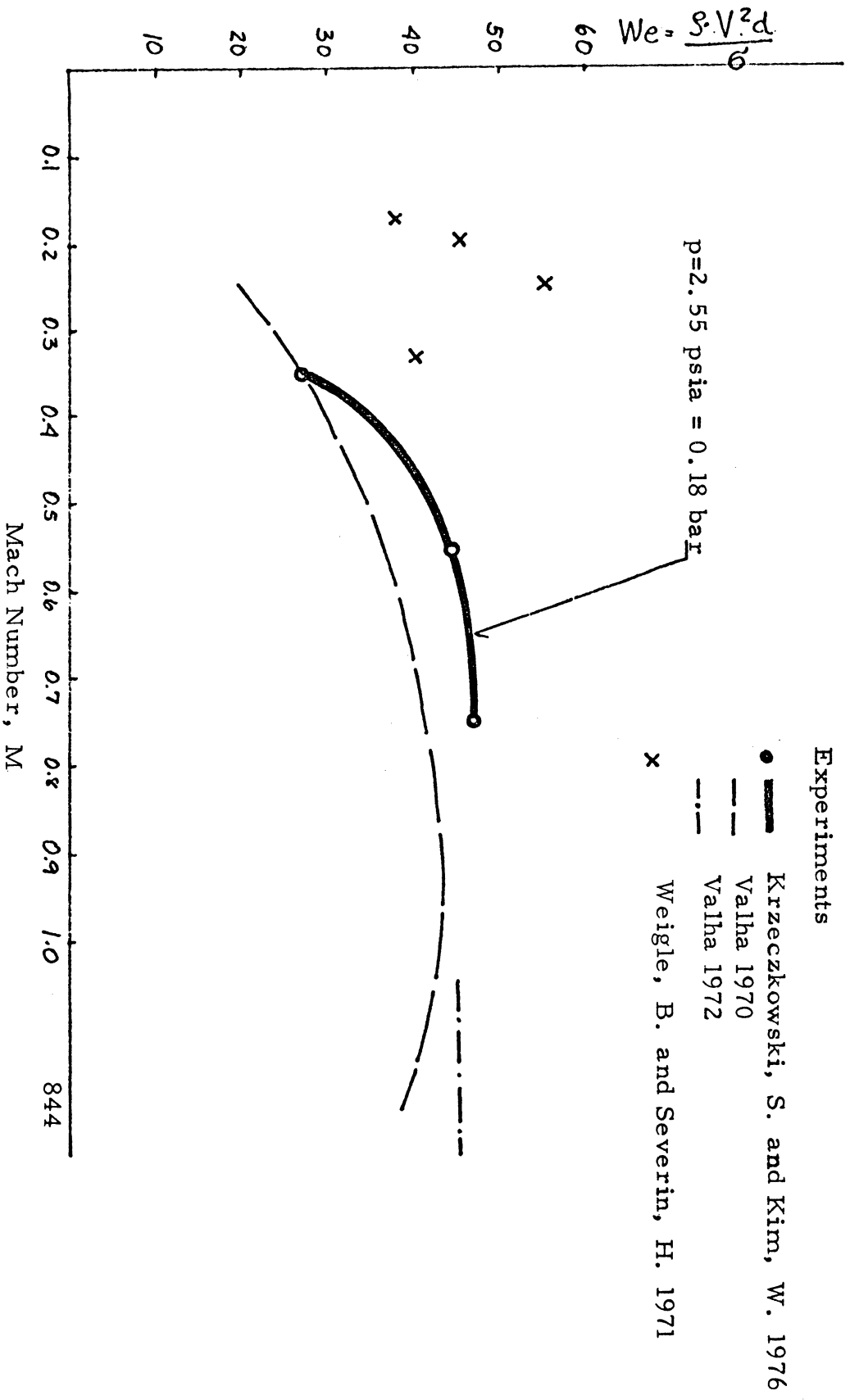


Figure 6 - The Weber Number of Maximum Droplets far Downstream From the Trailing Edge



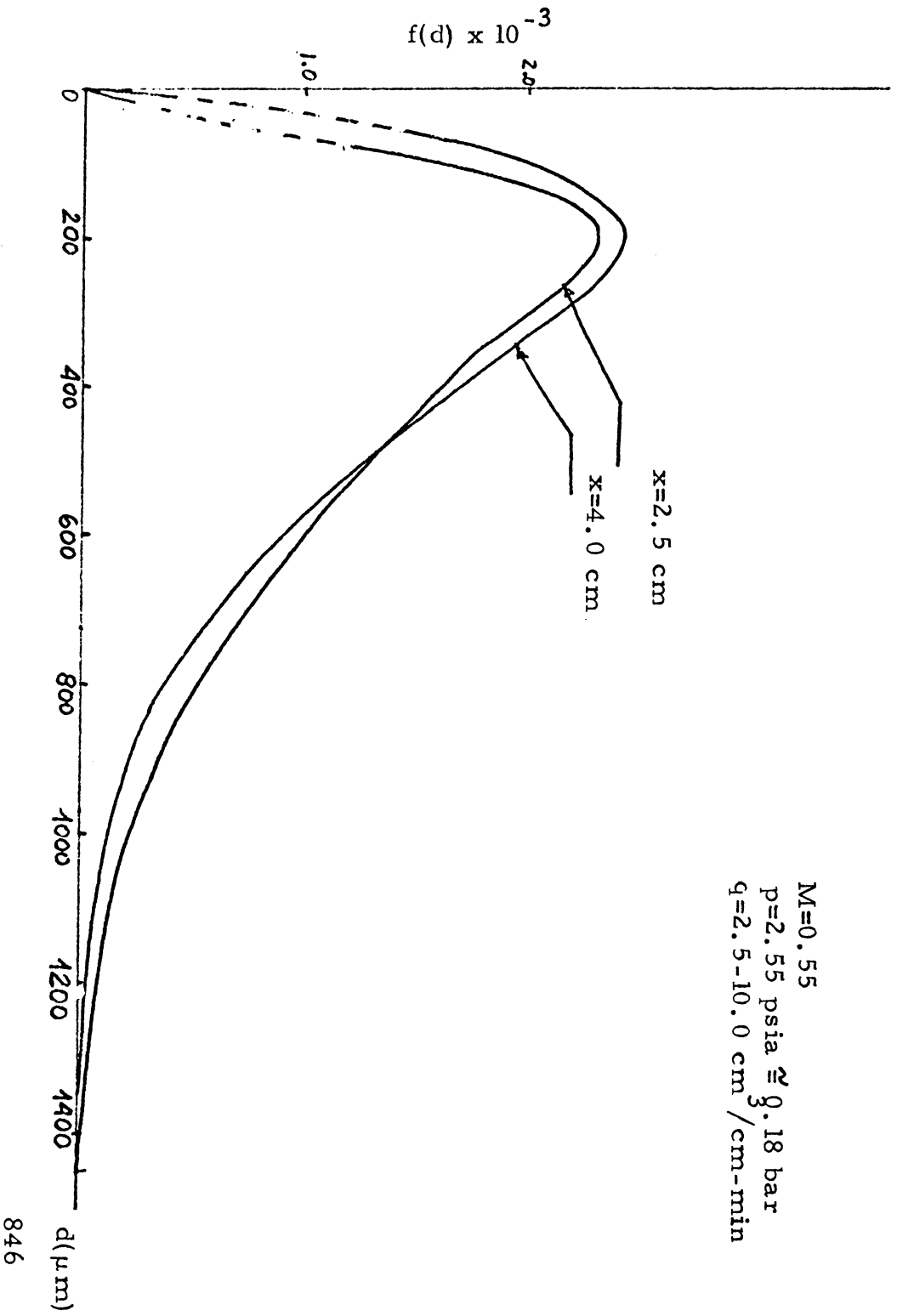
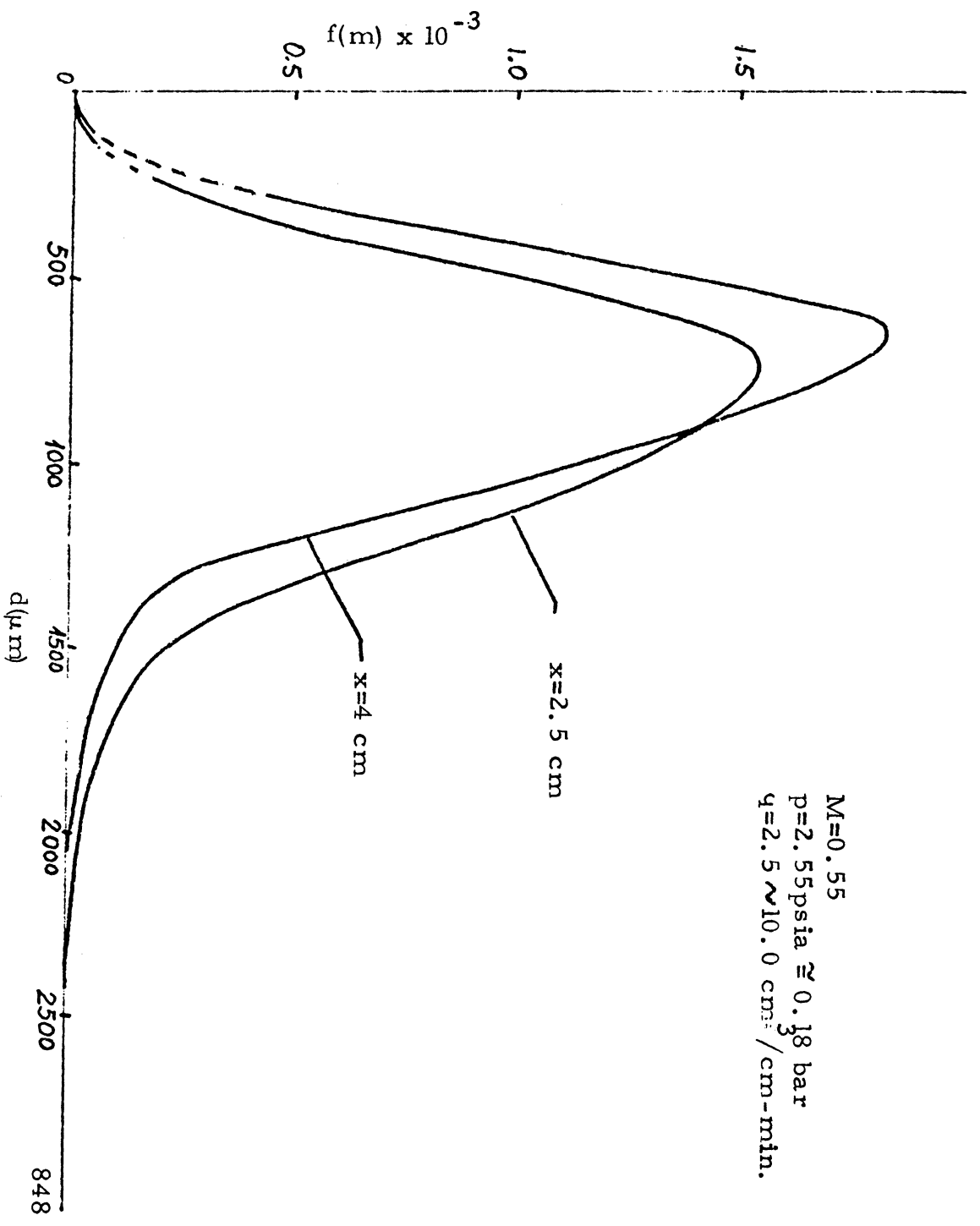


Figure 7 - Droplet Size Distribution Function at  $M = 0.55$ ,  
 $X = 2.5 \text{ cm}$  and  $X = 4.0 \text{ cm}$ .



$M=0.55$   
 $p=2.55 \text{ psia} \approx 0.18 \text{ bar}$   
 $q=2.5 \sim 10.0 \text{ cm}^3/\text{cm-min.}$

Figure 8 - Droplet Mass Distribution Function at  $M = 0.55$ ,  
 $X = 2.5 \text{ cm}$  and  $X = 4.0 \text{ cm}$ .

UNIVERSITY OF MICHIGAN  
3 9015 03466 5862